

Spreading of correlations and entanglement after a quench in the one-dimensional Bose-Hubbard model

Andreas M. Läuchli

Institut Romand de Recherche Numérique en Physique des Matériaux (IRRMA),
CH-1015 Lausanne, Switzerland

E-mail: laeuchli@comp-phys.org

Corinna Kollath

Centre de Physique Théorique, Ecole Polytechnique, CNRS, 91128 Palaiseau Cedex,
France

E-mail: kollath@cpht.polytechnique.fr

Abstract. We investigate the spreading of information in a one-dimensional Bose-Hubbard system after a sudden parameter change. In particular, we study the time-evolution of correlations and entanglement following a quench. The investigated quantities show a light-cone like evolution, i.e. the spreading with a finite velocity. We discuss the relation of this velocity to other characteristic velocities of the system, like the sound velocity. The entanglement is investigated using two different measures, the von-Neuman entropy and mutual information. Whereas the von-Neumann entropy grows rapidly with time the mutual information between two small sub-systems can as well decrease after an initial increase. Additionally we show that the static von Neuman entropy characterises the location of the quantum phase transition.

PACS numbers: 03.75.Lm 05.70.Ln 67.40.Fd73.43.Nq

1. Introduction

Entanglement and correlations are important properties of quantum systems. The interest in these quantities is manifold. Correlations have been used since a long time to characterize the low energy properties of quantum many body states. In particular in the study of quantum phase transitions, correlations played a leading role. Entanglement has been the resource for quantum computing and quantum cryptography. Only recently entanglement has also become a major tool to understand and characterize ground states of interacting quantum many body systems. Driven by these applications the study of entanglement has become an active field of research and many different measures have been proposed in quantum many body systems [1].

Recently the interest in the fundamental questions of quantum dynamics was reinforced by the experimental realization of strongly interacting gases [2]. In these systems the precise and rapid tunability of the system parameters and the very good decoupling from the environment open the possibility to study the quantum evolution of a system far from equilibrium. In this context the following questions arise: How does a quantum system react to a parameter change? How fast can information propagate through the system? How do correlations and entanglement between different parts of the system build up?

These and similar questions have been asked in different situations. Lieb and Robinson found for one-dimensional spin systems that the quantum dynamics generated by local operators obeys a light-cone like evolution, i.e. the information spreads with a finite velocity [3]. They proved that only exponentially small corrections exist outside this light-cone in the considered systems. Many generalizations of this Lieb Robinson theorem have been developed over the last years (see Ref. [4] and references therein). Further the finding of the spreading of correlations with a finite velocity after a global quench has been verified in specific integrable models [5, 6, 7, 8, 9], as well as for critical systems which can be described by conformal field theory [10, 11].

Motivated by the experimental investigation of a sudden parameter change across the superfluid to Mott-insulator transition [12] we investigate here the time-evolution of a one-dimensional non-integrable Bose-Hubbard system after a sudden quench of the interaction strength. For this model the recent generalization of the Lieb-Robinson theorem of Cramer et al. [4] applies deep in the superfluid regime. However, no generalization exists in the presence of sizable interaction strength between the bosons.

We start our investigation with the static properties of the von Neumann entanglement entropy in the Bose-Hubbard model. In particular we show that previous predictions from conformal field theory [13, 14] are in very good agreement with our numerical results in the critical superfluid phase assuming a central charge $c = 1$. We further point out how the knowledge on the dependence of the entanglement entropy on the system and block length in the critical phase can be used to locate the quantum phase transition.

We then turn to the discussion of the time-evolution of the quantum system after

a sudden parameter change. Hereby we mainly consider a quench from the superfluid to the Mott-insulating phase. However, we also show some examples of quenches inside the superfluid or the Mott-insulating regime. In a previous work [15] we focussed on the relaxation of the system to a quasi-stationary state after a quench. Here in contrast we discuss the short time behaviour in detail. We study the spreading of information by the time-evolution of correlations, the von Neumann entropy, and the mutual information. We find that for onsite quantities the time-scale of relaxation is set by the hopping time of the bosons. In contrast for longer range correlations, like the one-particle density matrix or the density-density correlations, a front spreads with almost constant velocity which causes a ‘light-cone’ like evolution. The front travels at a finite speed, such that in an infinite system equilibrium can never be reached. We discuss the time evolution of the von Neumann entropy of different contiguous blocks of length l . We find that the von Neumann entropy of a certain block shows a sharp linear rise for short time and saturates for longer times. To a good approximation the rate of the block entropy increase is shown to follow a boundary law, while the entropy value at saturation depends only on the block volume. Our results nicely corroborate recent analytical results [16, 17, 18]. In contrast to the von Neumann entanglement, the mutual information between two contiguous blocks of different length after a quench to a Mott-insulating regime drops substantially in time compared to the values in the initial superfluid state. So for the considered quench the growth of the entropy and the loss of correlations go hand in hand.

2. Model and methods

Ultracold bosons subjected to an optical lattice can be described by the Bose-Hubbard model [19, 20, 21], here in its one-dimensional form

$$H(J, U) = -J \sum_j \left(b_j^\dagger b_{j+1} + h.c. \right) + \frac{U}{2} \sum_j n_j (n_j - 1), \quad (1)$$

where b_j^\dagger and b_j are the boson creation and annihilation operators, and $n_j = b_j^\dagger b_j$ the number operators on site j . The first term in Equation (1) models the kinetic energy of the atoms and the parameter J is called the hopping parameter. The second term stems from the short range interaction between the atoms and the parameter U characterizes its strength. In the experimental setup of ultracold bosons in an optical lattice the parameters U and J can be directly related to the experimental parameters. In particular, by varying the lattice height in the experiment the parameter U/J can be changed by several orders of magnitude and by anisotropic lattices the dimensionality of the system can be varied. In equilibrium at integer filling the Bose-Hubbard model shows a quantum phase transition at a critical value of $u_c := (U/J)_c$ between a superfluid state ($U/J < u_c$), in which the atoms are delocalized, to a Mott insulating state ($U/J > u_c$) in which the atoms are localized [21]. We use $\hbar = 1$ and $a = 1$, where a denotes the lattice spacing, throughout the work. The theoretical tools we use to treat the

ground state and the dynamic properties of the Bose-Hubbard model are analytical approximations and numerical methods. Static results for the entanglement entropy are obtained using the density matrix renormalization group method (DMRG) [22, 23, 24] with up to 1000 states. The results for time-evolution are calculated using the exact diagonalization (ED) based on Krylov methods [25, 26] and the adaptive time-dependent DMRG (t-DMRG) [27, 28, 29]. The ED is used to study one-dimensional chains with periodic boundary conditions up to 16 sites, while the adaptive t-DMRG is used for one dimensional systems with open boundaries and with up to 64 sites keeping several hundred DMRG states.

3. Static von Neumann Entanglement Entropy

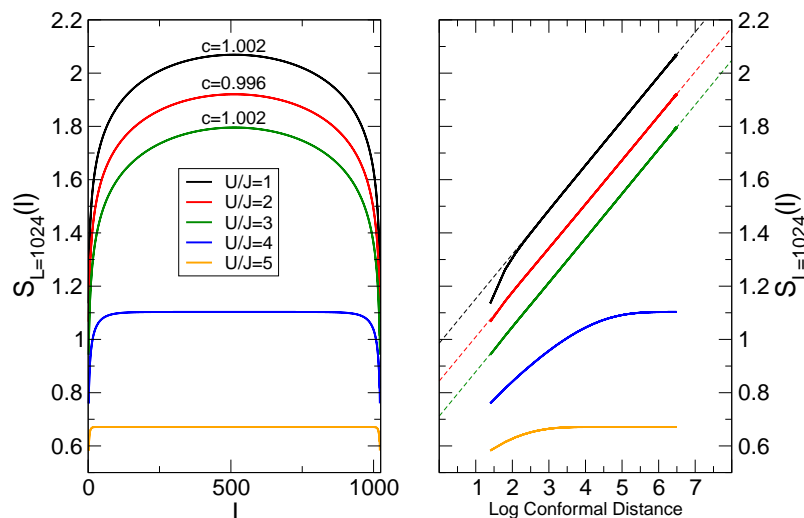


Figure 1. Left panel: The static von Neumann block entropy $S_L(l)$ for an open system of length $L = 1024$ and a range of different interaction values U/J , located in the superfluid and the Mott insulating phases. The average filling is $n = 1$. Right panel: the same data as a function of the logarithmic conformal distance $\lambda := \log[(2L/\pi) \sin(\pi l/L)]$. The linear behavior of the curves of $U/J = 1, 2$ and 3 reveals the $c = 1$ critical theory. The rapid saturation of the entropy for $U/J = 4$ and 5 is a consequence of the short correlation length in the Mott insulating phase.

Before we discuss the behaviour of the system after a sudden change of the parameters we would like to discuss the static properties of entanglement in the Bose-Hubbard model. In recent years many different measures have been proposed for the entanglement in a system [1]. One of the proposed measures is the von Neumann block entropy. Let A be a block of length l and B be the remaining system. Then the von Neumann entropy of a block A is defined by $S_A = -\text{Tr}_A \rho_A \log \rho_A$, where $\rho_A = \text{Tr}_B \rho$ is the reduced density matrix of the block A and $\rho = |\Psi\rangle\langle\Psi|$ the pure-state density matrix of the whole system. Tr_X denotes the trace over X .

In the superfluid phase the low energy physics of the one-dimensional Bose-Hubbard model can be described by a Luttinger liquid, which is a conformal field theory with

central charge $c = 1$. For such a 1+1 critical system the von Neumann entropy has been derived for different geometries of the subsystems A and B [13, 14]. If A is a single block of length l in a periodic system of length L the von Neumann entropy is given by

$$S_A = \frac{c}{3} \log \left[\frac{L}{\pi} \sin \left(\frac{\pi l}{L} \right) \right] + s_1. \quad (2)$$

Here s_1 is a non-universal constant. In a system with open boundary conditions which is divided at some interior point into an interval A of length l and its complement the von Neumann entropy is

$$S_L(l) = \frac{c}{6} \log \left[\frac{2L}{\pi} \sin \left(\frac{\pi l}{L} \right) \right] + \log g + s_1/2. \quad (3)$$

Here $\log g$ is the boundary entropy of Affleck and Ludwig [30]. Note that an oscillating correction term beyond the conformal field theory prediction (3) has been found for open boundary conditions in the critical phase of the $S = 1/2$ XXZ spin model [31]. This is a specific example of Friedel-like oscillations decaying away from the boundaries. These, in turn, lead to an oscillating, algebraically decaying correction term to the block entropy. In the case of the Bose Hubbard model considered here, which is not particle-hole symmetric, the open boundaries can induce a slightly non-uniform particle density, but the amplitude of the difference with respect to the nominal density decays rapidly away from the boundaries. The effect is most pronounced for small U/J and becomes negligible for large U/J . This inhomogeneous particle density distribution is therefore expected to affect the entanglement entropy on small open systems.

For stronger interactions the quantum phase transition to the Mott-insulating phase takes places. The Mott-insulating state is characterized by an energy gap above the ground state and has a finite correlation length ξ . For gapped systems with a finite correlation length ξ , the block entropy is expected to saturate at a finite value $S_L(l) \sim \log(\xi)$ for $l \gg \xi$ [32, 14].

We show in Fig. 1 the von Neumann entropy of the static Bose-Hubbard model with open boundary conditions for different interaction strengths U/J obtained using DMRG calculations on a system of length $L = 1024$. In the left panel we show the entropy as a function of the block length l , while in the right panel we rescale the x -axis according to the logarithmic conformal distance $\lambda := \log [(2L/\pi) \sin(\pi l/L)]$. Eq. 3 then simplifies as $S_L(\lambda) = c/6 \lambda + \log g + s_1/2$.

For small interaction strength $U/J = 1, 2, 3$ our results agree very well with the prediction (3) of the conformal field theory for large block length l . For $U/J = 1$ deviations at small l can be seen. They are due to the slightly inhomogeneous density in the open system. Linear fits to the curves in the right panel for the larger values of λ yield slopes which are very close to the expected value of $1/6$. The extracted value of c for the three critical U/J values is shown close to the corresponding curve in the left panel. The values of c are very accurately 1. The constant contribution $\log g + s_1/2$ becomes smaller for increasing U/J due to the reduced onsite number fluctuations. For $U/J = 4$ and 5 a very clear saturation of the entropy as a function of the block length l can

be seen, revealing the finite correlation length in the Mott insulator. The entanglement entropy vanishes completely in the limit of $U/J \rightarrow \infty$ when the groundstate becomes a trivial product wave function of singly occupied sites.

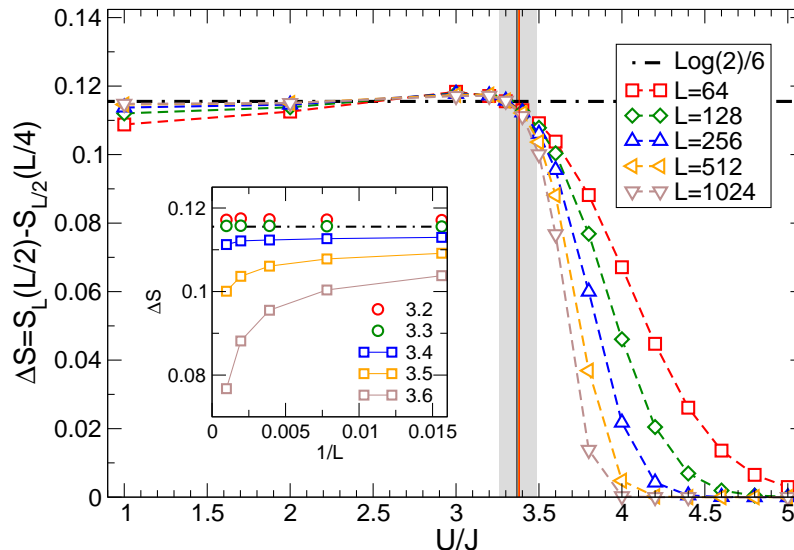


Figure 2. Difference $\Delta S(L) = S_L(L/2) - S_{L/2}(L/4)$ versus U/J for different system lengths L at average filling $n = 1$. For $U/J < u_c$ the expected scaling behaviour $\Delta S = c/6 \log 2$ with $c = 1$ is seen. In the $L \rightarrow \infty$ limit the data converges to a step function located at u_c . The vertical line shows the previously obtained critical values $u_c \approx 3.37(12)$ [33] (black line with grey uncertainty) and $u_c \approx 3.380(4)$ [34] (red line) for comparison. The deviation of small system length for $U \leq 2J$ stems from inhomogeneous density distribution due to the open boundaries and is not captured in the CFT approach. Inset: ΔS as a function of $1/L$ for selected values of U/J close to the phase transition.

In the following we investigate whether it is possible to locate the critical value u_c purely based on the properties of the von Neumann entropy. Earlier high precision work with DMRG mostly used a priori knowledge about the Kosterlitz-Thouless transition to accurately locate the critical value [33, 34]. A recent investigation based on quantum information related quantities such as the fidelity and single site entropies and their derivatives arrived at the conclusion that the single site entropy would not allow to locate the critical value u_c precisely [35].

In order to locate the critical point we devise the quantity

$$\Delta S(L) := S_L(L/2) - S_{L/2}(L/4) \quad (4)$$

the increase of the entropy at the mid-system interface upon doubling the system size. In a region of parameter space described by a conformal field theory with central charge c one expects simply $\Delta S = c/6 \log 2$ based on Equation (3). On the other hand in a gapped region with a finite correlation length one obtains $\Delta S = 0$ for $L \gg \xi$, because the entropy saturates for block lengths l larger than the correlation length ξ . As the system size increases one therefore expects ΔS for the one-dimensional Bose-Hubbard model to scale to a step function as a function of U/J .

In Figure 2 we display ΔS as a function of U/J for different system sizes L from 32 up to 1024 sites. In the Luttinger liquid regime at small U/J the curves for different system sizes nicely converge towards the expected value of $1/6 \log 2$. For larger U/J values the ΔS curves scale to zero for increasing L , indicative of the gapped phase. Based on our available data we can safely infer that the point $U/J = 3.4$ is already in the Mott insulating phase, while $U/J = 3.3$ is still critical, see inset of Figure 2. This result is in full agreement with the previously obtained critical values $u_c \approx 3.37(12)$ [33] and $u_c \approx 3.380(4)$ [34], based on fits of the decaying bosonic Green's function. In future studies using a fine grid of U/J values one could perform a finite size scaling of the inflection point to extract an even more accurate value of u_c . So we conclude that an appropriate scaling plot of the von Neumann entanglement entropy provides competitive results on the location of the quantum phase transition in the one-dimensional Bose Hubbard model without relying on a priori knowledge of the Kosterlitz-Thouless nature of the transition.

4. Description of the parameter quench

We implement the quench by an abrupt change of the interaction strength from an initial value U_i to a final value U_f at fixed hopping parameter J at time $t = 0$. In most cases we start from a superfluid phase ($U_i/J < u_c$) and change to the Mott-insulating regime ($U_f/J > u_c$). The initial wave function $|\psi_0\rangle$ for $t \leq 0$ is the ground state of the Hamiltonian $H_i = H(J, U_i)$. We investigate its time evolution for times $t > 0$ subject to the Hamiltonian $H_f = H(J, U_f)$. The time evolution of the wave function is governed by the Schrödinger equation, i.e.

$$|\Psi(t)\rangle = \exp(-iH_f t) |\Psi_0\rangle.$$

The time evolution of expectation values of relevant operators can be expressed as

$$\langle \hat{O}(t) \rangle = \sum_{m, m'} c_m^* c_{m'} \exp[-i(E_m - E_{m'})t] \langle m | \hat{O} | m' \rangle. \quad (5)$$

Hereby $|m\rangle$ are the eigenstates of the final Hamiltonian H_f and E_m the corresponding energy eigenvalues. The expansion of the initial state $|\psi_0\rangle$ into the eigenstates of the final Hamiltonian, i.e. $|\psi_0\rangle = \sum_m c_m |m\rangle$ with the weights c_m , is used. In a realistic case the tunneling between lattice sites and the interaction strength are non-zero and to determine the time-evolution of the wave function is not an easy task. We calculated the time-evolution numerically using ED and DMRG methods and analytical approximation in certain limits.

5. Light cone effect in correlations

In this section we investigate how correlations over a distance r react to the sudden parameter change. We consider two different types of correlations, the single particle

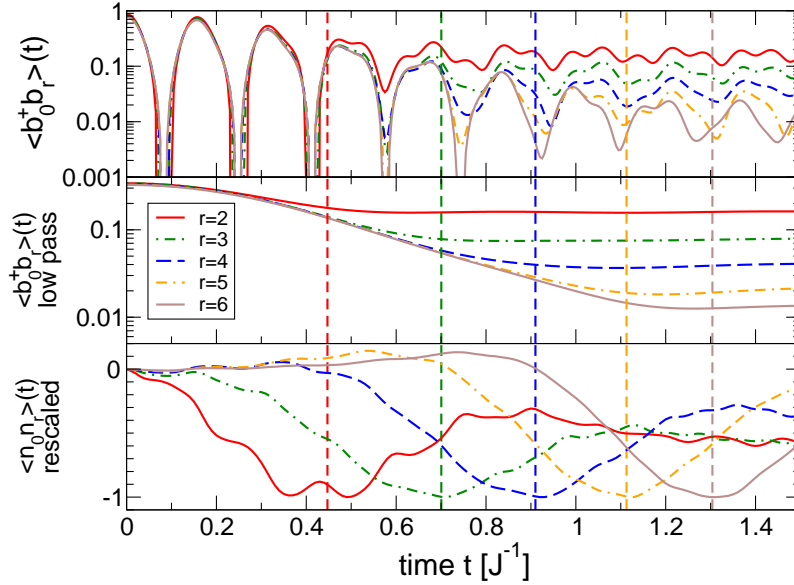


Figure 3. Time-evolution of correlation functions after a quench from $U_i = 2J$ to $U_f = 40J$. The upper panel shows the single particle correlation functions $\langle b_0^\dagger b_r \rangle$ for different distances r . The correlations show partial revivals up to a time t_r when they start to reach a quasi-steady state. This time t_r grows approximately linearly with the distance r as marked by the vertical lines. The central panel shows the same correlations functions after filtering out the high frequencies, see text for details. The lowest panel shows the density density correlations function $\langle n_0 n_r \rangle$ after shifting and rescaling their amplitude for better visibility. The common vertical dashed lines denote the arrival of the minima as determined from the density-density correlations. The data shown is ED for a $L = 14$ and DMRG data for $L = 32$ and filling $n = 1$.

correlations $\langle b_j^\dagger b_{j+r} \rangle$ and the density-density correlations $\langle n_j n_{j+r} \rangle$ at equal time. In Fig. 3 we show the time-evolution of the different correlations after a quench from the superfluid, $U_i = 2$, to the Mott-insulating, $U_f = 40$, parameter regime.

Single-particle correlations The upper panel shows the correlations $\langle b_0^\dagger b_r \rangle$ for different distances r †. For short times the single particle correlations oscillate with the period $2\pi/U_f$. The origin of these oscillations lies in the integer spectrum of the operator $\hat{n}_j(\hat{n}_j - 1)/2$. Consider the limit of very strong interactions, where the time-evolution is totally dominated by the interactions. The time evolution of the single particle correlations is given by

$$\langle b_i^\dagger b_j \rangle(t) = \sum_{\{m\}, \{m'\}} \delta_{m_i, m'_i+1} \times \delta_{m_j, m'_j-1} \times e^{iU_f(m'_j - m'_i - 1)t} c_m^* c_{m'} \langle \{m\} | b_i^\dagger b_j | \{m'\} \rangle.$$

Here we use the notation $\{m\}$ for the Fock state with m_i particles on site i . The time-evolution of the correlation function is determined by the non-vanishing cross terms

† To extract these correlations from the DMRG data with open boundary conditions the average over central sites is taken. Note that for periodic boundary conditions this quantity is real due to symmetry, whereas for open boundary conditions an imaginary part can develop. However for the shown functions and times the imaginary part is negligible.

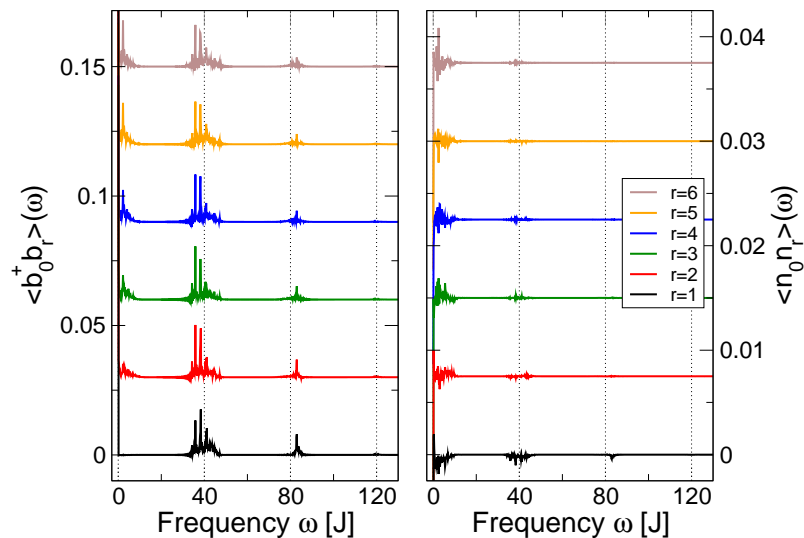


Figure 4. Fourier transform of the equal-time single-particle and density-density correlation functions for different distances r . The same parameters as in Figure 3 are used. In the single-particle correlation function clear frequency bands located at multiples of the interaction strength $U_f = 40J$ can be seen. The density-density correlation is dominated by the contributions at low frequencies from zero up to $\sim J$.

$\langle \{m\} | b_i^\dagger b_j | \{m'\} \rangle$ of Fock states whose occupations vary by removing one particle from site j and adding it at site i . The frequencies occurring in the time-evolution will be given by $U_f(m'_j - m'_i - 1)$. This results in oscillations of period $T \approx 2\pi/U_f$ for equally occupied lattice sites j and i of the state $|\{m'\}\rangle$. For unequal onsite occupations higher multiples of U_f can occur in the frequency spectrum.

Thus the distribution of the different frequencies in the Fourier transformation of the single particle correlation functions (left panel in Fig. 4) and the occupation difference in the initial state are intimately connected. For the shown quench ($U_i = 2J, U_f = 40J$) sizable contributions of the lowest three frequency bands can be seen, whereas the occupation of higher frequency bands becomes very small. The distribution among the frequency bands changes by varying the initial value of the interaction strength U_i . If the initial state is deep in the superfluid regime, the peaks at higher frequencies show more weight due to the presence of strong particle number fluctuations. In contrast if the initial state is close to the Mott-insulating transition the particle fluctuations are suppressed and the weight of the peaks at higher frequencies decreases accordingly. The width of the frequency bands is due to the finite value of J and is responsible for the decay of the oscillations in time [15].

Let us now come back to the real-time evolution of the single particle correlations for different distances. After a time $t \approx 0.5/J$ the correlation corresponding to the smallest distance shown, $r = 2$, reaches a quasi-steady value (marked by the leftmost vertical line). The correlations of distance $r = 3$ deviate from the correlation with $r > 3$ for a time $t \approx 0.7/J$ (second left vertical line). The same can be observed for correlations with increasing distances at longer times. In the central part of the Figure 3 the same

single particle correlations are shown, but the high frequency oscillations at frequencies $\omega_n \sim n \times U_f$ with $n \gtrsim 1$ are filtered out, and only the $n = 0$ contributions are kept. In these low-pass filtered correlations the saturation to a quasi-steady state value can be seen much more clearly.

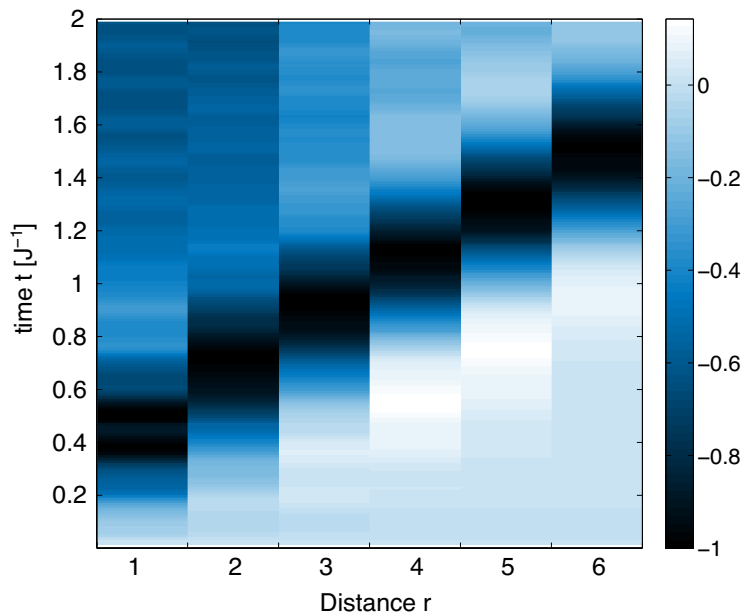


Figure 5. Time-evolution of the rescaled density-density correlations $\langle n_0 n_r \rangle(t)$ after a quench with the same parameters as in Figure 3. The front of the evolution evolves approximately with a constant velocity.

Density-density correlations The lowest panel of Figure 3 shows the density-density correlations $\langle n_j n_{j+r} \rangle - \langle n_j \rangle \langle n_{j+r} \rangle$ at equal time. The amplitudes of the correlations are rescaled and shifted for better readability §.

The density-density correlations do not show strong oscillations, but remain almost constant in time up to the moment, where a pronounced signal arrives. In their Fourier spectrum (right panel of Figure 4) mostly low frequencies $\sim J$ occur. This is due to the fact that the interaction term of the Hamiltonian commutes with the correlation function. Thus, in the strong coupling limit the interaction term does not give rise to oscillations. Approximately at the same time as the single particle correlations saturate, the spreading of a signal (here the reaching of a minimum, loci of the common vertical dashed lines in Figure 3) can be found in the density-density correlation $\langle n_0 n_r \rangle$.

In Figure 5 we show a contour plot of the rescaled density correlations. In this representation a clear light cone evolution can be seen, i.e. a front travels through the system at almost constant speed. Let us note, that the same light cone effect occurs in

§ We will denote the rescaled function $\langle n_j n_{j+r} \rangle - \langle n_j \rangle \langle n_{j+r} \rangle$ averaged over different sites j in the center of the chain by $\langle n_0 n_r \rangle$.

the evolution of the correlations for different quench parameters (cf. Table 1) and also in incommensurate systems, e.g. at filling $n = 1/2$.

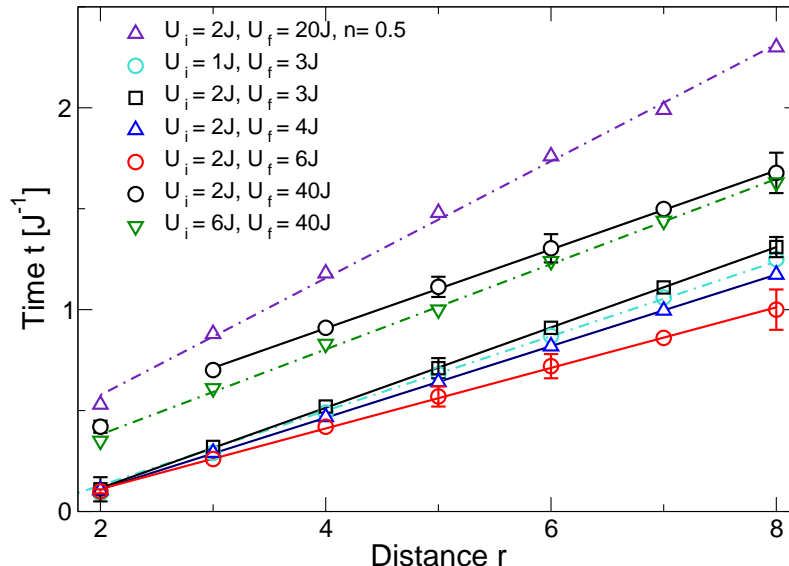


Figure 6. Characteristic time t_r for arrival of the signal in the density-density correlations depending on the distance r are summarized for different quench parameter U_i , U_f , and average density n . A clear linear relation between time and distance is observed for all shown quenches. To give an order of the uncertainties, typical error bars are plotted for chosen points. They take into account both the difficulty to identify a sharp signal and deviations between different system length ($L = 14$ up to $L = 64$).

Propagation velocity v_s To extract the velocity v_s of the signal propagation in the density-density correlations, we plot in Figure 6 the time t_r , when a signal, e.g. the minimum, occurs in the density-density correlations versus the distance r . The curves for different values of the initial and final interaction strength U_i and U_f are presented. A clear linear behaviour of the time t_r versus the distance is seen. The shift between the curves, e.g. for $U_f = 20, 40$ and $U_f = 4, 6$, stems from the different signatures that have been tracked in the density-density correlations. The inverse of the slope is the signal propagation velocity v_s of the signature. We extract the velocity v_s by a linear fit $t_r = r/v_s + b$, where v_s and b are the fitting parameters. The results for v_s are shown in Table 1.

The velocity of the spreading of correlations after a quench has been identified by Calabrese and Cardy [10] within conformal field theory and for different integrable models to be twice the maximal mode velocity. The simple picture given is that the modes depart from both considered sites and the signal arrives, if both modes interfere. In the description by a conformal field theory this velocity agrees with the sound velocity of the system, since the dispersion relation is linear. In a chain of harmonic oscillators or in a spin chain lattice effects occur, which cause a curved dispersion relation. Thus the maximal velocity of a mode can be distinct from the sound velocity in the system.

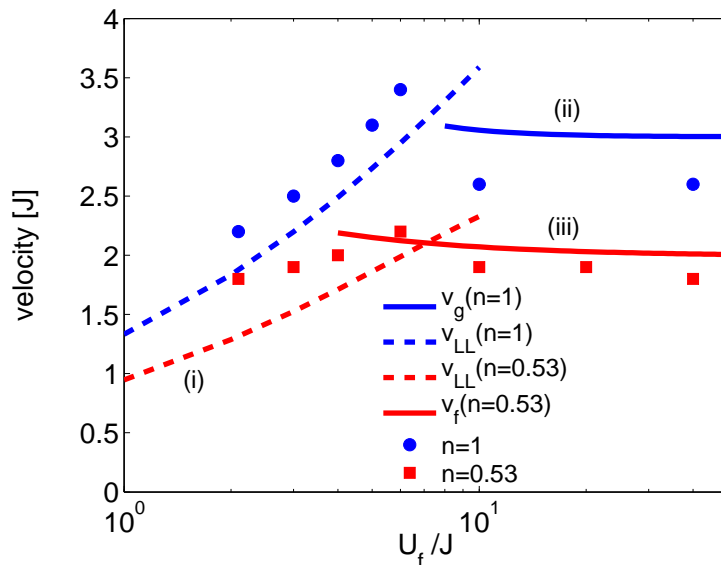


Figure 7. Dependence of the velocity $v_s/2$ on the final interaction strength after the quench. Results are shown for different values of the density and compared to an analytical approximation described in the text. The initial value is $U_i = 2J$.

Table 1. Velocity extracted from a linear fit.

n	U_i/J	U_f/J	$v_s[J]$
1	2	2.1	4.4
1	2	3	5
1	2	4	5.6 ± 0.4
1	2	5	6.2
1	2	6	6.8
1	2	10	5.2
1	2	40	5.2 ± 0.6
1	1	4	5.9
1	3	4	5.6
1	6	40	4.8
1	1	3	5.2

n	U_i/J	U_f/J	$v_s[J]$
0.5	2	2.1	3.6
0.5	2	3	3.8
0.5	2	4	4
0.5	2	6	4.4
0.5	2	10	3.8
0.5	2	20	3.8
0.5	2	40	3.6

For the transverse Ising model a velocity equal to one has been found [5].

In Figure 7 we show the results for the rescaled signal velocity $v_s/2$ for one initial interaction strength $U_i = 2J$. We present results for different densities. At the commensurate density $n = 1$ a phase transition to the Mott-insulator takes place at a critical value. In contrast for the incommensurate density $n = 1/2$ || the system stays in the superfluid phase for all interaction strengths. The signal velocity shows a strong increase for low interaction strength. After reaching a maximum around $U/J \approx 6$ it saturates for strong interactions to an almost constant value.

|| In the open $L = 32$ system used in the t-DMRG, the density in the middle of the system is $n \approx 0.53$.

We further compare our results to different characteristic velocities of the Bose-Hubbard model: (i) the sound velocity in the superfluid regime, (ii) the maximal mode velocity of a simplified model in the Mott-insulator, (iii) the maximal mode velocity of a fermionic model applicable at low filling.

(i) For an infinitesimal quench inside the superfluid phase, the rescaled signal velocity $v_s/2$ for the spreading of the correlations can be described by the sound velocity of the system. However, for finite quenches we expect the rescaled signal velocity to be larger than the sound velocity, since modes with higher velocities can be excited. In Figure 7 we approximate the sound velocity in the superfluid regime by the sound velocity of the corresponding continuous Lieb-Liniger model [36]. For small values of γ , it is given by $v_{LL} = 2n\sqrt{\gamma}\sqrt{1 - \frac{\sqrt{\gamma}}{2\pi}}$, where $\gamma = U/(2Jn)$. This expression approximates the sound velocity for the Bose-Hubbard model up to an interaction strength $\gamma \lesssim 4$ [37].

(ii) An idea of the expected signal velocity in the Bose-Hubbard model in the Mott-insulating state can be obtained by mapping the system onto a simpler model using only three local states, e.g. occupation by $n_0 - 1$, n_0 , and $n_0 + 1$ bosons per site, where n_0 is an integer [38, 39]. In the Mott-insulating phase the dispersion relation for a particle hole excitations in this effective model can be determined as $\epsilon(k) = \sqrt{U^2 - U\epsilon_0(k)(4n_0 + 2) + \epsilon_0(k)^2}/2$ [39]. Here $\epsilon_0(k) = 2J \cos(ka)$ is the band dispersion for the non-interacting case. The group velocity in this case is given by $v = \frac{\partial\epsilon(k)}{\partial k}$. The maximum velocity v_g of a mode given by this model is shown in Figure 7. In the strong coupling limit this velocity agrees with the velocity extracted from a perturbative calculation where the maximal group velocity is given by $aJ/\hbar(2n_0 + 1)$. For the case of $n = 1$ this results in $3aJ/\hbar$. In particular we see that towards the critical value in this model the velocity slightly increases. The momentum at which the maximum velocity is reached changes compared to the strong coupling limit.

(iii) For strong interaction and low filling the Bose-Hubbard system can be mapped onto a fermionic system [40]. In this fermionic system the velocity is given by $v_f = 2 \sin(\pi n)(1 - 8Jn \cos(\pi n)/U)$.

In Figure 7 we compare our numerical results to the different velocities (i)-(iii). For small interaction strength we see that the velocity $v_s/2$ is always larger than the sound velocity showing a similar rise with U/J . Comparing further the velocity of different quenches in the superfluid regime, e.g. $U_i = 1, 2$ and $U_f = 4$ in Table 1, the velocity $v_s/2$ seems to approach the sound velocity if the parameter changes becomes smaller.

In the regime of strong interaction the qualitative features of the signal velocity are well reproduced by the given approximations. In particular, the velocity is almost constant for high interaction values and increases if U/J is lowered towards $U/J \approx 6$. Further the order of magnitude of the values is in good agreement.

However, the approximation has to be taken with care. It does not take all higher energy excitations into account, which will be necessary to quantitatively describe the situation under consideration. Further it does not take into account the initial state, i.e. which of the modes are actually excited by the quench. This is in contrast to the numerical results in Table 1 which suggest that the value of the observed signal velocity

might depend as well on the initial state. In particular if the higher particle fluctuations are present in the initial state the observed signal velocity seems to be larger.

6. Dynamics of entanglement and mutual information

We turn in the following to the time-evolution of the entanglement and the amount of correlations between different subsystems after a quench. As a measure for the entanglement we use the von Neumann block entropy (see section 3) and the mutual information. Whereas the von Neumann entropy describes the entanglement of a region of the system with the remaining part, the mutual information gives a measure about the amount of correlations between different subsystems [41]. In the following we first analyze the time-evolution of the von Neumann entropy before we turn to the evolution of the mutual information.

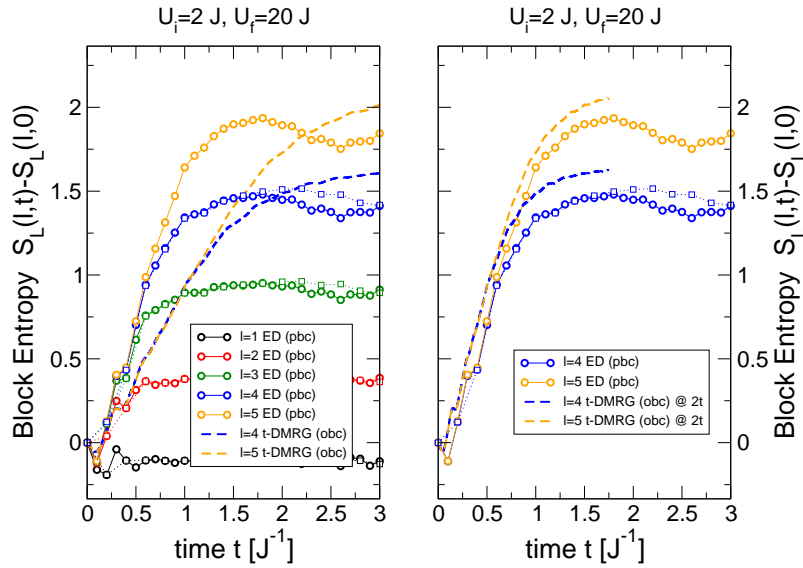


Figure 8. Time-evolution of the block entropy for different block lengths for a quench from $U_i = 2J$ to $U_f = 20J$. The initial linear rise is the same for different block lengths, but depends on the boundary condition of the block (PBC: two interface links per block, faster rise of the entropy; OBC: one interface link per block, slower rise of the entropy). For longer times a saturation of the entropy depending linearly on the block length is observed. The left panel contains the original time evolution, while in the right panel, the obc data has been plotted for times $\tilde{t} = 2t$, so as to illustrate the slower increase of the entropy due to the smaller boundary. The PBC results are from ED on $L = 14$ (circles) and $L = 16$ (squares) systems, while the OBC data has been obtained using t -DMRG up to $L = 64$.

von Neumann entropy In Fig. 8 we show the time-evolution of the von Neumann entropy for Bose-Hubbard systems with periodic (ED, $L = 14, 16$ ¶) and open boundary

¶ Due to the computational challenge of calculating density matrices in ED for large blocks we chose to limit the local boson occupancy to 3 at most.

conditions (t-DMRG, 5 bosons per site are allowed). In both cases we focus on contiguous blocks of length l . For open boundary conditions the blocks are aligned with one of the boundaries. We plot the difference $S_L(l, t) - S_L(l, 0)$ so that the curves for all block sizes start at zero at $t = 0$.

In the left panel we show data for ED ($l = 1, 2, 3, 4, 5$) and DMRG ($l = 4, 5$) results for a specific quench from $U_i = 2J$ to $U_f = 20J$. Let us first discuss the ED results: Immediately after the quench for $t \lesssim 0.4J^{-1}$ a small dip shows up in all block entropies. However, from time $t \approx 0.4\hbar/J$ up to $t^*(l)$ a linear rise of the block entropies can be observed. Interestingly all block sizes for $l > 1$ have the same slope, until they bend over to an almost flat behaviour at successively later times. The dip in the entropy at larger times is a finite size effect, as can be seen by comparing the data for different system sizes (circles for $L = 14$ and squares for $L = 16$). The saturation value of the different block entropies depends linearly on the block size, defining an entropy propagation velocity v_e , which is roughly equal to v_s determined based on the density-density correlation functions in the preceding section 5. In a next step it is instructive to compare the entanglement dynamics between different block geometries (two interface links in ED, one interface link in t-DMRG). The t-DMRG results are also shown in the left panel of Figure 8. The entropy of these open blocks increases more slowly, but converges to about the same value at late times as the periodic blocks of the same length. To illustrate this convincingly we show in the right panel the same data, but where the entropy of the open blocks is shown on a time scale which is twice as fast. Indeed the results of the two block geometries agree reasonably well. This nice result lends direct support to the picture developed by Calabrese and Cardy [16], where they predicted that the saturation of the entropy occurs at $t_{\text{PBC}}^*(l) = l/2v$ for periodic boundary conditions, while $t_{\text{OBC}}^* = l/v$ for blocks aligned with an open boundary.

These characteristics of the entanglement evolution are similar to the results obtained for different models in Refs. [16, 42, 43, 17, 1, 44]. A linear growth of the entropy has been seen up to times $t = l/2v$, where v is the maximal velocity of the excitations. Afterwards a saturation of the entropy is seen for $t \rightarrow \infty$, and the rate of the approach to the saturation value is related to the dispersion relation of the underlying model. At a fixed time the entanglement saturates for increasing block length, i.e. fulfills a boundary law with the boundary increasing with time. This shows that the boundary law for the dynamics of entanglement which has been proven mostly for 1D spin-systems [17, 18] seems to be valid in more general systems such as the Bose-Hubbard system considered here.

Mutual information While the von Neumann entropy is rapidly increasing in time and finally leads to an extensive entropy scaling with the block volume at large times, it is interesting to ask whether the vast entanglement entropy also leads to increased correlations between subparts of the system. A very useful quantity to address this question is the mutual information. The mutual information $I(A : B)$ between two

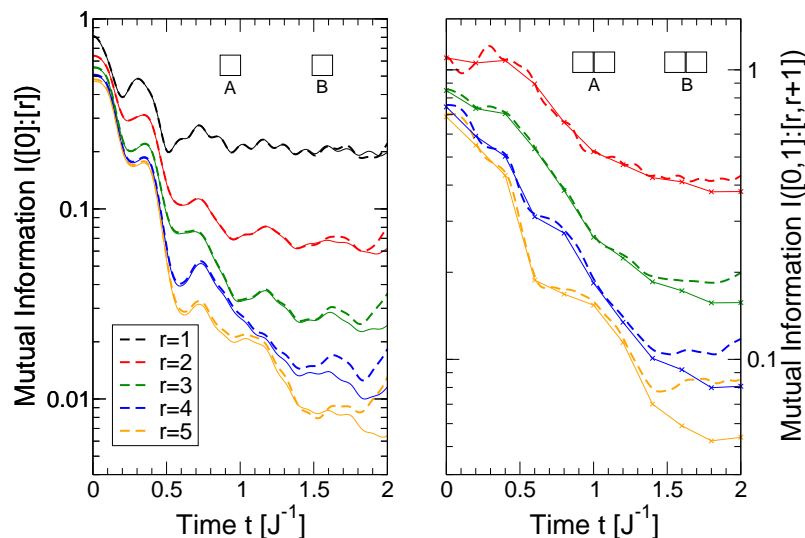


Figure 9. (Color online) Time-evolution of the mutual information (6) between two blocks of equal length $l = 1$ (left panel) and $l = 2$ (right panel) for different spatial separations r . The quench parameters are $U_i = 2J$, $U_f = 20J$, and $n = 1$. The results have been obtained by ED for $L = 14$ (bold, dashed lines) and $L = 16$ (thin, straight lines).

subsystems A and B of the system is defined by

$$I(A : B) = S_A + S_B - S_{A \cup B}. \quad (6)$$

Here S_X is the von Neumann entropy for the subsystem X . The mutual information $I(A : B)$ measures the total amount of information of system A about system B [41]. Note that $A \cup B$ is not required to be equal to the total system. Interestingly the mutual information can fulfill an area law at finite temperatures, while the entropy is expected to follow a volume law [45]⁺.

In Figure 9 we show the time evolution of the mutual information between two blocks of $l = 1$ (left panel) or $l = 2$ (right panel) sites each, shifted by a distance r . At $t = 0$ we expect the mutual information to decay slowly with the block separation r , since the starting state is basically a scale invariant critical state and the mutual information is just a complicated function of the basic critical correlation functions, such as $\langle b_0^\dagger b_r \rangle$ and $\langle n_0 n_r \rangle$, which all decay algebraically. As a function of time t , the mutual information is decreasing rapidly with some slow oscillations on top. For later times it seems as though the mutual information levels off to a finite value at a time which depends again linearly on the distance r . The mutual information at late times decays much faster as a function of distance than in the initial state. So even though the entanglement entropy is vastly growing in time, this does not lead to enhanced entanglement between different subsystems.

⁺ In this reference the authors study the case of the total system equal to $A \cup B$.

7. Conclusion

In our work we show that correlations and entanglement are very useful quantities to characterize the equilibrium and dynamic properties of a quantum many body system.

In the first part of our work we showed that the static von Neumann entanglement signals the quantum phase transition between the superfluid and Mott-insulating state without previous knowledge on the type of the phase transition. In the superfluid, the von Neuman entropy is in very good agreement with previous predictions by conformal field theory [13, 14] with a central charge $c = 1$. Deviation are only found close to the boundaries of the system. These deviations are induced by the inhomogeneous density distribution caused by the open boundary conditions. A saturation of the entropy with the block length is found in the gapped Mott-insulating phase as predicted [32, 14].

In the second part of our work, the time-evolution after a sudden parameter change is analyzed with a focus on the spreading of information. Hereby different parameter changes are discussed ranging from the change between the superfluid to Mott-insulating phase over a quench inside the superfluid to a quench inside the Mott-insulating regime. Our study proposes that the Lieb Robinson theorem is valid as well in the considered situation of the Bose-Hubbard model. This relies on our findings that a light-cone like evolution takes place in different correlation functions. The velocity of the front evolving in the correlation functions is discussed and compared to different characteristic velocities of the system. The validity of the Lieb-Robinson theorem is further supported by the von Neumann entropy which shows for a certain block length a linear growth for short times. To a good approximation the rate of the block entropy increase is shown to follow a boundary law, while the entropy value at saturation seems only to depend on the block volume. Our results nicely corroborate recent analytical results [16, 17, 18]. However, in contrast to the von Neumann entropy after a quench from the superfluid to the Mott-insulating regime, the mutual information between two spatially separated small blocks relaxes to a lower value than in the starting state. So even though the entanglement entropy is vastly growing in time, this does not necessarily lead to enhanced entanglement between different regions of the system.

8. Acknowledgement

We would like to thank E. Altman, J. Eisert, S. Huber, S. Manmana, A. Muramatsu, R. Noack, A. Rosch, and S. Wessel for fruitful discussions. This work was partly supported by the Swiss National Science Foundation. We wish to thank the Institute Henri Poincare-Centre Emile Borel for hospitality and support. Further CK acknowledges support by the RTRA network 'Triangle de la Physique' and the DARPA OLE program.

The ED simulations have been performed on the machines of the CSCS (Manno).

References

- [1] Luigi Amico, Rosario Fazio, Andreas Osterloh, and Vlatko Vedral. Entanglement in many-body systems. *Rev. Mod. Phys.*, 2008.
- [2] I. Bloch, J. Dalibard, and W. Zwerger. Many-body physics with ultracold gases. *arXiv:0704.3011*, 2007.
- [3] E. H. Lieb and D. W. Robinson. The finite group velocity of quantum spin systems. *Communications in Mathematical Physics*, 28:251–257, 1972.
- [4] M. Cramer, A. Serafini, and J. Eisert. Locality of dynamics in general harmonic quantum systems. *arXiv:0803.0890*, 2008.
- [5] F. Iglói and H. Rieger. Long-range correlations in the nonequilibrium quantum relaxation of a spin chain. *Phys. Rev. Lett.*, 85:3233, 2000.
- [6] Marcos Rigol, Alejandro Muramatsu, and Maxim Olshanii. Hard-core bosons on optical superlattices: Dynamics and relaxation in the superfluid and insulating regimes. *Physical Review A (Atomic, Molecular, and Optical Physics)*, 74(5):053616, 2006.
- [7] M. A. Cazalilla. Effect of suddenly turning on interactions in the luttinger model. *Physical Review Letters*, 97(15):156403, 2006.
- [8] T.S. Cubitt and J.I. Cirac. Engineering correlation and entanglement dynamics in spin systems. *quant-ph/0701053*, 2007.
- [9] M. Cramer, C. M. Dawson, J. Eisert, and T. J. Osborne. Exact relaxation in a class of nonequilibrium quantum lattice systems. *Physical Review Letters*, 100(3):030602, 2008.
- [10] Pasquale Calabrese and John Cardy. Time dependence of correlation functions following a quantum quench. *Phys. Rev. Lett.*, 96(13):136801, 2006.
- [11] Pasquale Calabrese and John Cardy. Quantum quenches in extended systems. *J.Stat.Mech.*, P008, 2007.
- [12] M. Greiner, O. Mandel, T. Esslinger, T. W. Hänsch, and I. Bloch. Quantum phase transition from a superfluid to a Mott insulator in a gas of ultracold atoms. *Nature*, 415:39, 2002.
- [13] C. Holzhey, F. Larsen, and F. Wilczek. Geometric and renormalized entropy in conformal field theory. *Nucl. Phys. B*, 424:44, 1994.
- [14] Pasquale Calabrese and John Cardy. Entanglement entropy and quantum field theory. *J. Stat. Mech.: Theor. Exp.*, P06002, 2004.
- [15] C. Kollath, A.M. Läuchli, and E. Altman. Quench dynamics and non-equilibrium phase diagram of the Bose-Hubbard model. *Phys. Rev. Lett.*, 98:180601, 2007.
- [16] Pasquale Calabrese and John Cardy. Evolution of entanglement entropy in one-dimensional systems. *J. Stat. Mech.: Theor. Exp.*, P04010, 2005.
- [17] Jens Eisert and Tobias J. Osborne. General entanglement scaling laws from time evolution. *Phys. Rev. Lett.*, 97(15):150404, Oct 2006.
- [18] S. Bravyi, M. B. Hastings, and F. Verstraete. Lieb-Robinson bounds and the generation of correlations and topological quantum order. *Phys. Rev. Lett.*, 97(5):050401, 2006.
- [19] D. Jaksch, C. Bruder, I. Cirac, C. W. Gardiner, and P. Zoller. Cold bosonic atoms in optical lattices. *Phys. Rev. Lett.*, 81(15):3108, 1998.
- [20] W. Zwerger. Mott-Hubbard transition of cold atoms in optical lattices. *Journal of Optics B.*, 5:9, 2003.
- [21] M. P. A. Fisher, P. B. Weichman, G. Grinstein, and D. S. Fisher. Boson localization and the superfluid-insulator transition. *Phys. Rev. B*, 40(1):546, 1989.
- [22] S. R. White. Density matrix formulation for quantum renormalization groups. *Phys. Rev. Lett.*, 69:2863, 1992.
- [23] K. Hallberg. New trends in density matrix renormalization. *Adv. Phys.*, 55:477, 2006.
- [24] U. Schollwöck. The density-matrix renormalization group. *Reviews of Modern Physics*, 77(1):259, 2005.
- [25] Tae Jun Park and J. C. Light. Unitary quantum time evolution by iterative lanczos reduction.

- J. Chem. Phys.*, 85(10):5870–5876, 1986.
- [26] Salvatore R. Manmana, Alejandro Muramatsu, and Reinhard M. Noack. Time evolution of one-dimensional quantum many body systems. *AIP Conf. Proc.*, 789:269, 2005.
- [27] G. Vidal. Efficient simulation of one-dimensional quantum many-body systems. *Phys. Rev. Lett.*, 93:040502, 2004.
- [28] S. R. White and A. E. Feiguin. Real time evolution using the density matrix renormalization group. *Phys. Rev. Lett.*, 93:076401, 2004.
- [29] A. J. Daley, C. Kollath, U. Schollwöck, and G. Vidal. Time-dependent density-matrix renormalization-group using adaptive effective Hilbert spaces. *J. Stat. Mech.: Theor. Exp.*, P04005, 2004.
- [30] Ian Affleck and Andreas W. W. Ludwig. Universal noninteger “ground-state degeneracy” in critical quantum systems. *Phys. Rev. Lett.*, 67(2):161–164, Jul 1991.
- [31] Nicolas Laflorencie, Erik S. Sorensen, Ming-Shyang Chang, and Ian Affleck. Boundary effects in the critical scaling of entanglement entropy in 1d systems. *Physical Review Letters*, 96(10):100603, 2006.
- [32] G. Vidal, J. I. Latorre, E. Rico, and A. Kitaev. Entanglement in quantum critical phenomena. *Phys. Rev. Lett.*, 90:227902, 2003.
- [33] T. D. Kühner, S. R. White, and H. Monien. One-dimensional Bose-Hubbard model with nearest-neighbor interaction. *Phys. Rev. B*, 61(18):12474, 2000.
- [34] Jakub Zakrzewski and Dominique Delande. Accurate determination of the superfluid-insulator transition in the one-dimensional bose-hubbard model. *arXiv:0701739*, 2007.
- [35] P. Buonsante and A. Vezzani. Ground-state fidelity and bipartite entanglement in the bose-hubbard model. *Physical Review Letters*, 98(11):110601, 2007.
- [36] E. H. Lieb. Exact analysis of an interacting Bose gas. II. the excitation spectrum. *Phys. Rev.*, 130:1616, 1963.
- [37] C. Kollath, U. Schollwöck, J. von Delft, and W. Zwerger. One-dimensional density waves of ultracold bosons in an optical lattice. *Phys. Rev. A*, 71:053606, 2005.
- [38] E. Altman and A. Auerbach. Oscillating superfluidity of bosons in optical lattices. *Phys. Rev. Lett.*, 89:250404, 2002.
- [39] S. D. Huber, E. Altman, H. P. Buchler, and G. Blatter. Dynamical properties of ultracold bosons in an optical lattice. *Physical Review B (Condensed Matter and Materials Physics)*, 75(8):085106, 2007.
- [40] M. A. Cazalilla. Are the Tonks regimes in the continuum and on the lattice truly equivalent? *Phys. Rev. A*, 70:041604(R), 2004.
- [41] Berry Groisman, Sandu Popescu, and Andreas Winter. Quantum, classical, and total amount of correlations in a quantum state. *Physical Review A (Atomic, Molecular, and Optical Physics)*, 72(3):032317, 2005.
- [42] Luigi Amico, Andreas Osterloh, Francesco Plastina, Rosario Fazio, and G. Massimo Palma. Dynamics of entanglement in one-dimensional spin systems. *Physical Review A (Atomic, Molecular, and Optical Physics)*, 69(2):022304, 2004.
- [43] G. De Chiara, S. Montangero, P. Calabrese, and R. Fazio. Entanglement entropy dynamics in Heisenberg chains. *J. Stat. Mech.*, page P03001, 2006.
- [44] Peter Barmettler, Ana Maria Rey, Eugene Demler, Mikhail D. Lukin, Immanuel Bloch, and Vladimir Gritsev. Quantum many-body dynamics of coupled double-well superlattices. *arXiv:0803.1643*, 2008.
- [45] Michael M. Wolf, Frank Verstraete, Matthew B. Hastings, and J. Ignacio Cirac. Area laws in quantum systems: mutual information and correlations. *Phys. Rev. Lett.*, 100:070502, 2008.